Modulation analysis of nonlinear beam refraction at an interface in liquid crystals

Modulation analysis of nonlinear beam refraction at an interface in liquid crystals

Gaetano Assanto,[1] Noel F. Smyth,[2] and Wenjun Xia[2]

[1]*NooEL—Nonlinear Optics and OptoElectronics Lab,University of Rome "Roma Tre," Via della Vasca Navale 84, 00146 Rome, Italy*

[2]*School of Mathematics and Maxwell Institute for Mathematical Sciences, University of Edinburgh, Edinburgh EH9 3JZ, Scotland, United Kingdom*

(Received 18 June 2011; published 13 September 2011)

A theoretical investigation of solitary wave refraction in nematic liquid crystals is undertaken. A modulation theory based on a Lagrangian formulation of the governing optical solitary wave equations is developed. The resulting low-dimensional equations are found to give solutions in excellent agreement with full numerical solutions of the governing equations, as well as with previous experimental studies. The analysis deals with a number of types of refraction from a more to a less optically dense medium, the most famous being the Goos-Hänchen shift upon total internal reflection.

DOI: 10.1103/PhysRevA.84.033818 PACS number(s): 42.65.Tg, 42.70.Df, 05.45.Yv

I. INTRODUCTION

Nematic liquid crystals have been proven to be an ideal medium in which to study nonlinear light beam propagation due to their "giant" nonlinearity, so that nonlinear effects can be observed over millimeter distances and at milliwatt power levels. Nematic liquid crystals possess a self-focusing, intensity-dependent response, so that optical solitary waves, termed nematicons, can form due to a balance between the nonlinear refractive index increase and diffraction [1–3]. While two-dimensional solitary waves governed by nonlinear Schrödinger (NLS)-type equations are usually unstable to "catastrophic" collapse in a finite length [4], nematic liquid crystals are an example of a nonlocal dielectric in which solitary waves are stabilized because the medium response extends far beyond the waist of the exciting optical beam [2,3].

Several proposed applications of nematicons, such as switches and routers, are based on controlling their trajectory [5–15], e.g., by altering the refractive index distribution in the liquid crystalline sample. This can be achieved in a number of ways, including the use of an external low-frequency electric field [8,16,17] and/or extra optical beams to perturb the solitary wave environment [5,7,9–15]. The present work will be concerned with nematicon control and steering through index changes caused by an external low-frequency or static electric field (voltage).

Extensive theoretical studies of one-dimensional solitary wave refraction and reflection at an interface were carried out for local [18] and nonlocal media [19] by Aceves *et al*. These studies used both numerical beam propagation solvers and asymptotic solutions based on the equivalent particle approximation [20], which provided results in good agreement with numerical solutions. Most studies of refraction of spatial solitary waves at interfaces have dealt with bright solitary waves. However, dark and grey solitary waves in self-defocusing dielectrics also show refraction at interfaces separating media with different optical properties [21,22].

The present work investigates the refraction and (total internal) reflection of nematicons at an (straight) interface between regions in a liquid crystal cell with different molecular director orientations, and therefore different refractive indices and walk-off, as in earlier experimental studies [16,23,24]. These regions can be formed by applying two unequal external, low-frequency biases, which results in two background pretilt orientations of the director. The refraction and reflection are studied using both full numerical solutions of the nonlocal equations governing the propagation of a nematicon and a modulation theory based on their Lagrangian formulation [25]. This modulation theory is related to the equivalent particle method [18–20]; in fact, it is the same in the limit in which the input beam is a slowly varying nematicon; that is, its amplitude and waist satisfy the relation for a steady nematicon [2]. Modulation theory possesses the advantage that it gives good agreement with numerical [25] and experimental [17] results even if the beam's amplitude and waist are not given by the steady-state relation. It uses appropriate trial functions for the unknown nematicon profile; however, in many applications, the nematicon trajectory is independent of the details of the trial profile [11,14,15,26]. Besides allowing for unknown solitary wave solutions and wider profile variations, the present work studies nematicon refraction in two space dimensions, at variance with the one-dimensional work of Aceves *et al*. [18,19]. It also includes the background dependent walk-off of the extraordinary polarized nematicon beam. In the case of propagation from a more to a less optically dense medium, total internal reflection can occur, as expected. This reflection is nonspecular and can take a number of forms, in agreement with experiments [16,23,24] and theory [18]. The nematicon can penetrate the less dense medium, but still turn and reenter the more dense medium again, the Goos-Hänchen or lateral shift [27]. For higher angles of incidence, a large portion of the beam remains in the optically denser medium, only its tail entering the less dense medium. Eventually not enough of the tail enters the less dense medium to result in significant deviation of the beam trajectory.

II. MODULATION EQUATIONS

Let us consider a thick layer (several optical wavelengths) of uniaxial nematic liquid crystals (NLC) occupying a planar cell, with boundary conditions arranged such that the optic axis or molecular director belongs to the plane xz everywhere in the cell. The cell is configured so that two independent biasing static, external electric fields can be applied across its thickness [16] and adjust, by reorientation, the angle between the optic axis and the direction z down the cell. A coherent

beam of light is then launched into the cell and propagates in the volume of nonlinear dielectric. Let us define a coordinate system such that the applied electric fields are in the x direction (i.e., across the NLC thickness), the same direction as the polarization of the extraordinary input beam launched in the principal plane xz. The transverse direction y completes the right-hand coordinate system. In the paraxial approximation the nondimensional equation governing the envelope of the input extraordinary polarized light beam is [2,3,28]

$$i\frac{\partial E}{\partial z} - i\Delta\frac{\partial E}{\partial y} + \frac{1}{2}\nabla^2 E + [\sin^2\psi - \sin^2\psi_b]E = 0. \quad (1)$$

The angle ψ is the angle the NLC molecular director makes with the z axis, while ψ_b is the pretilt angle due to the external bias and can be nonuniform. The walk-off angle δ between the Poynting vector and the wave vector of the extraordinary beam is given by

$$\Delta = \tan\delta = \frac{\Delta n^2 \sin 2\psi}{\Delta n^2 + 2n_\perp^2 + \Delta n^2 \cos 2\psi}, \quad (2)$$

where $\Delta n^2 = n_\parallel^2 - n_\perp^2$ is the optical birefringence and $n_\parallel$ and $n_\perp$ are the refractive indices for fields parallel and perpendicular to the optic axis, respectively [28]. For full three dimensional propagation of a nematicon, the walk-off Δ is the projection of the walk-off onto the observation plane yz [23]. The Laplacian ∇^2 operates in the (x,y) plane.

The input beams used in experiments have milliwatt power levels [1], so that the reorientation of the NLC due to light is substantially less than that due to the bias field(s). Let us then take $\psi = \psi_b + \theta$, where $|\theta| \ll |\psi_b|$. In this limit, a Taylor series expansion in the electric field equation (1) results in

$$i\frac{\partial E}{\partial z} - i\Delta\frac{\partial E}{\partial y} + \frac{1}{2}\nabla^2 E + \sin(2\psi_b)\theta E = 0 \quad (3)$$

to first order in $|\theta|$. In a similar manner, the nondimensional equation governing the director orientation is

$$\nu\nabla^2\theta - 2q\theta = -\sin(2\psi_b)|E|^2 \quad (4)$$

to first order in $|\theta|$ [2,3,29]. Here ν measures the elastic response of the NLC. The usual experimental operating regime has ν large, $\nu = O(100)$, the so-called nonlocal regime in which the NLC response extends far beyond the beam waist. The parameter q is proportional to the square of the static electric field [2,3]. While the system of Eqs. (3) and (4) has been derived in the context of nonlinear beam propagation in nematic liquid crystals, it is general and describes nonlinear propagation in a diverse range of media for which the nonlinearity is accompanied by some diffusive phenomena [18].

To complete the description of the NLC cell and the equations governing the propagation of the extraordinary beam, the external bias configuration of the cell needs to be specified. The geometry assumed will be the same as for the experimental setup of Peccianti *et al.* [16,24] for which the two different static fields were applied through thin film electrodes with a straight gap separating them. This gap lies at a slope in the (y,z) plane and can be described by $y = \mu_1 z + \mu_2$. The change in biasing field, and therefore the change in the pretilting angle, is modeled with a sharp discontinuity. This is consistent with experiments for which the electric field was found to vary smoothly between two constant values over a distance of the order of the gap between the electrodes, of about 50 μm [23,24]. Hence the background pretilt is approximated by

$$\psi_b = \begin{cases} \psi_{\rm bl}, & \mu_1 z + \mu_2 < y, \\ \psi_{\rm br}, & y < \mu_1 z + \mu_2, \end{cases} \quad (5)$$

and q takes the two values

$$q = \begin{cases} q_l, & \mu_1 z + \mu_2 < y, \\ q_r, & y < \mu_1 z + \mu_2. \end{cases} \quad (6)$$

The simplified nematicon equations, Eqs. (3) and (4), do not possess an exact solitary wave solution, even in the case when ψ_b and q are constant. To obtain an analytical model for nematicon evolution, a modulation theory based on suitable trial functions for the electric field and director distribution profiles has been found useful [25] and is employed here. The nematicon equations (3) and (4) have the Lagrangian

$$L = i(E^*E_z - EE_z^*) - i\Delta(E^*E_y - EE_y^*) - |\nabla E|^2 + 2\sin(2\psi_b)\theta|E|^2 - \nu|\nabla\theta|^2 - 2q\theta^2. \quad (7)$$

Suitable trial functions for the electric field and director distribution [25] are

$$E = a\,\mathrm{sech}\,\frac{\sqrt{x^2+(y-\xi)^2}}{w}\,e^{i\sigma+iV(y-\xi)} + ige^{i\sigma+iV(y-\xi)},$$
$$\theta = \alpha\,\mathrm{sech}^2\,\frac{\sqrt{x^2+(y-\xi)^2}}{\beta}. \quad (8)$$

Here a and w are the amplitude and waist of the nematicon, α and β are the amplitude and width of the director distribution, ξ is the nematicon position (beam axis), V is the propagation constant, giving the angle of propagation of the nematicon in the (y,z) plane, and σ is the nematicon phase. The parameter g measures the height of the shelf of low wave number diffractive radiation which accumulates under the solitary wave as it evolves [25,30]. An input beam evolves to a steady-state nematicon through the shedding of conserved quantities via radiation; this shelf does not remain flat, but matches into diffractive radiation propagating away from the nematicon. Hence g is assumed to be nonzero in the disk of radius R, $0 \leqslant \sqrt{x^2+(y-\xi)^2} \leqslant R$, centered on the nematicon. All the nematicon parameters are functions of z. In the nonlocal limit the diffractive radiation shed by a nematicon has a significant effect on its evolution only for large values of z [25]; however, as propagation is considered hereby for $z = O(10)$, the effect of this shed radiation is ignored in the present work.

Substituting the trial functions (3) and (4) into the Lagrangian (7) and averaging by integration in x and y from $-\infty$ to ∞ results in the averaged Lagrangian [31]

$$\mathcal{L} = -2(I_2a^2w^2 + \Lambda g^2)\left[\sigma' - V\xi' - \frac{1}{2}V^2\right] - 2I_1aw^2g' + 2I_1w^2ga' + 4I_1awgw' - I_{22}a^2 - 4\nu I_{42}\alpha^2 + \frac{A^2B^2\alpha\beta^2a^2w^2}{2Q}[\sin(2\psi_{\rm bl})\,\mathrm{erfc}(\lambda_1) + \sin(2\psi_{\rm br})\,\mathrm{erfc}(-\lambda_1)]$$

$$+\frac{1}{2}B^2a^2w^2V[\Delta_l\,\mathrm{erfc}(\lambda_2)+\Delta_r\,\mathrm{erfc}(-\lambda_2)]$$
$$-\frac{1}{4}D^2\alpha^2\beta^2[q_l\,\mathrm{erfc}(\lambda_3)+q_r\,\mathrm{erfc}(-\lambda_3)]. \quad (9)$$

Here $\Delta_l=\Delta(\psi_{\mathrm{bl}})$, $\Delta_r=\Delta(\psi_{\mathrm{br}})$, and $\mathrm{erfc}(\zeta)$ is the complementary error function [32]. The arguments of the complementary error functions are

$$\lambda_1=\frac{\sqrt{A^2\beta^2+B^2w^2}}{AB\beta w}(\mu_1 z+\mu_2-\xi),$$
$$\lambda_2=\frac{\mu_1 z+\mu_2-\xi}{Bw},\quad \lambda_3=\frac{\sqrt{2}(\mu_1 z+\mu_2-\xi)}{D\beta}, \quad (10)$$
$$Q=A^2\beta^2+B^2w^2.$$

Finally, the various integrals I_i and I_{ij} appearing in this averaged Lagrangian are given in Appendix B and $\Lambda=R^2/2$, the area of the shelf of low wave number radiation under the beam, modulo 2π. Taking variations of this averaged Lagrangian with respect to the parameters results in the modulation equations governing the refraction of the self-confined beam at the interface. These modulation equations are given in Appendix A.

III. RESULTS AND COMPARISON WITH NUMERICAL SOLUTIONS

The nematicon equations (3) and (4) were solved using the pseudospectral method of Fornberg and Whitham [33]. In order to eliminate spurious numerical effects, the discontinuities in ψ_b and q across $y=\mu_1 z+\mu_2$ were smoothed using $\tanh(y-\mu_1 z-\mu_2)/w_t$ to link the orientations ψ_{bl} and ψ_{br} and q_l and q_r. For small w_t this smoothing made no difference to the solutions, other than to eliminate unphysical beam deformations and possible splitting, which occurred as $w_t\to 0$. As noted in the previous section, in experiments the pretilting field and the background director distribution

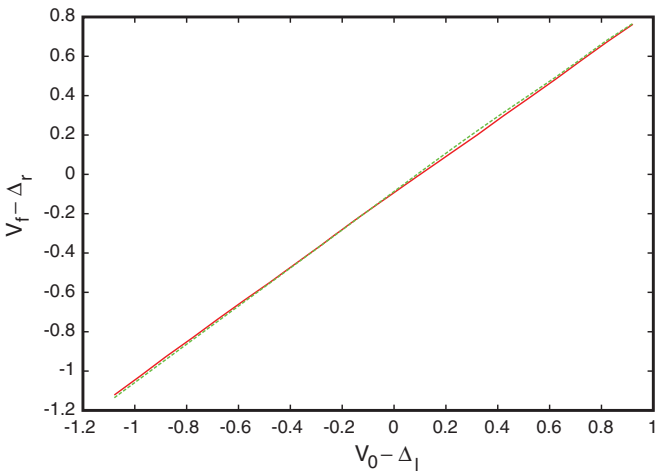

FIG. 1. (Color online) Comparison of refracted propagation constant $V_f-\Delta_r$ versus incident propagation constant $V_0-\Delta_l$ as given by the full numerical and modulation solutions. The parameter values are $a=4.5$ and $w=2.5$, with $\nu=200$, $\psi_{\mathrm{bl}}=0.4$, $\psi_{\mathrm{br}}=0.9$, $q_l=1.0$, $q_r=1.3$, $\mu_1=2$, and $\mu_2=-20$. Numerical solution,—(solid red line); modulation solution,– – –(dashed green line).

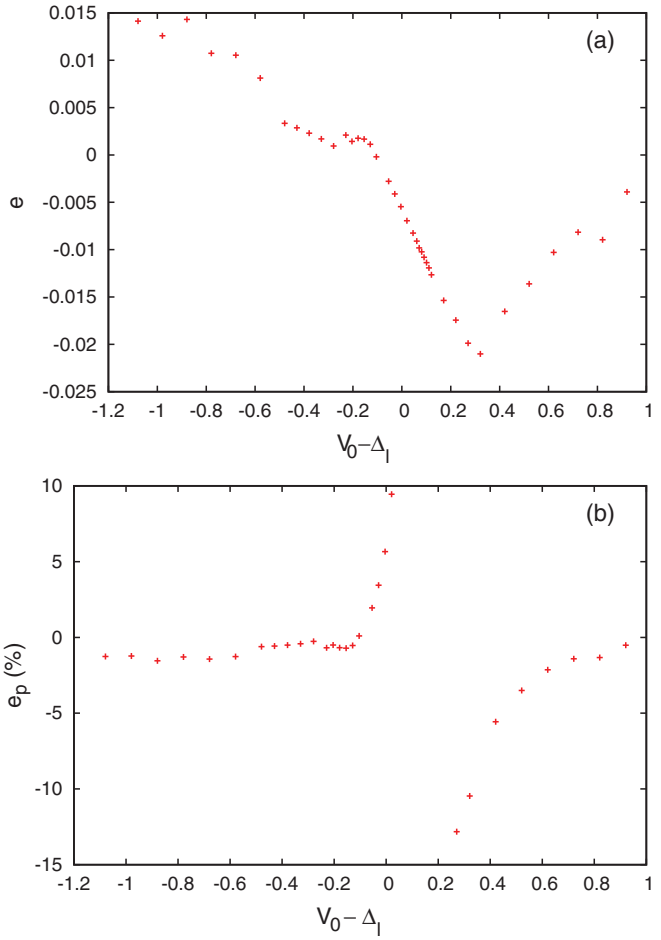

FIG. 2. (Color online) The error in the refracted propagation constant $V_f-\Delta_r$ as given by the modulation theory compared with the numerical solution as a function of incident propagation constant $V_0-\Delta_l$. The parameter values are $a=4.5$ and $w=2.5$, with $\nu=200$, $\psi_{\mathrm{bl}}=0.4$, $\psi_{\mathrm{br}}=0.9$, $q_l=1.0$, $q_r=1.3$, $\mu_1=2$, and $\mu_2=-20$. (a) Error e. (b) Percentage error e_p.

varied smoothly, and rapidly, between the two constant values [23,24]. Therefore, smoothing this change for the numerical solution is more appropriate than applying boundary conditions at the interface, as in previous studies of two media with different properties separated by an interface [18,19]. The modulation equations of Appendix A were solved using the standard fourth-order Runge-Kutta method.

In the experiments of Peccianti *et al.* [16] the angle of refraction of the nematicon was changed by varying the relative voltage difference between the two portions of the NLC cell across the interface. In the present work the relative voltage difference is kept constant for each case of propagation into higher and lower optically dense media. The angle of refraction will be changed by varying the input angle of the beam, i.e., the angle of incidence. In this context, it should be noted that changing the angle of the interface is equivalent to changing the incidence angle of the nematicon. The values of the background director angle ψ_b and the other parameter values were chosen to be within the experimental ranges [16].

Let us first consider a typical case of a nematicon propagating from a less to a more optically dense medium. Figure 1

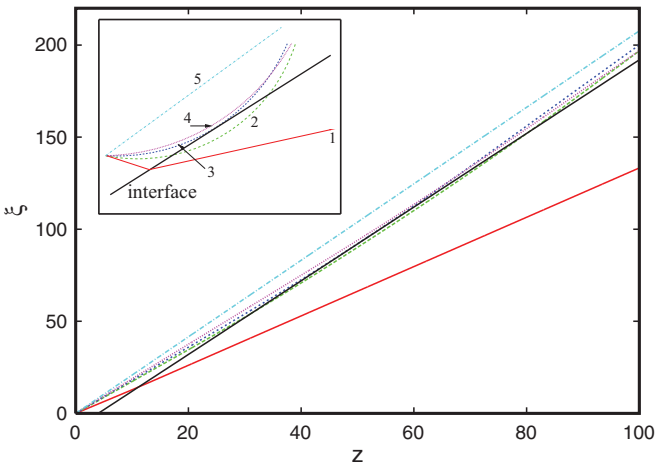

FIG. 3. (Color online) Beam behavior types as it propagates from more to less optically dense medium. Inset shows schematic of possible beam trajectories. 1, refraction,—(solid red line); 2, Goos-Hänchen type reflection,— — —(long dash green line); 3, total internal reflection at the interface,– – –(short dash dark blue line); 4, total internal reflection with beam axis in more dense medium, ··· (dotted pink line); 5, unchanged beam path,– - – - –(dash dot light blue line). The interface is the thick straight solid line (black).

shows a comparison between the final propagation constant as a function of the input propagation constant as given by the full numerical and modulation solutions. V_0 refers to the input value of V and V_f refers to the steady value after passing the interface. The propagation constant is the tan of the angle that the tangent to the beam trajectory makes with the z axis. It can be seen that the modulation equations give results in excellent agreement with the numerical solutions for a wide range of input angles. This is further confirmed by the difference between the modulation value of $V_f - \Delta_r$ and the

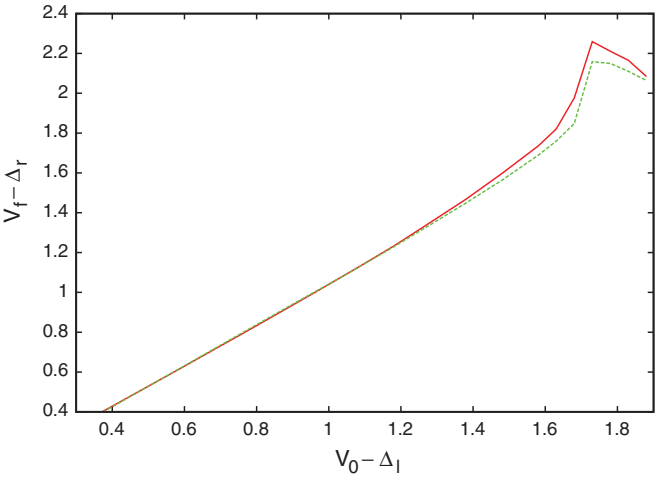

FIG. 4. (Color online) Comparison of the refracted propagation constant $V_f - \Delta_r$ versus incident propagation constant $V_0 - \Delta_l$ as given by the full numerical and modulation solutions, respectively. The parameter values are $a = 5$ and $w = 2$, with $\nu = 200$, $\psi_{\rm bl} = 0.8$, $\psi_{\rm br} = 0.6$, $q_l = 1.3$, $q_r = 1.0$, $\mu_1 = 2.0$, and $\mu_2 = -8.0$. Numerical solution,—(full red line); modulation solution,– – –(dashed green line).

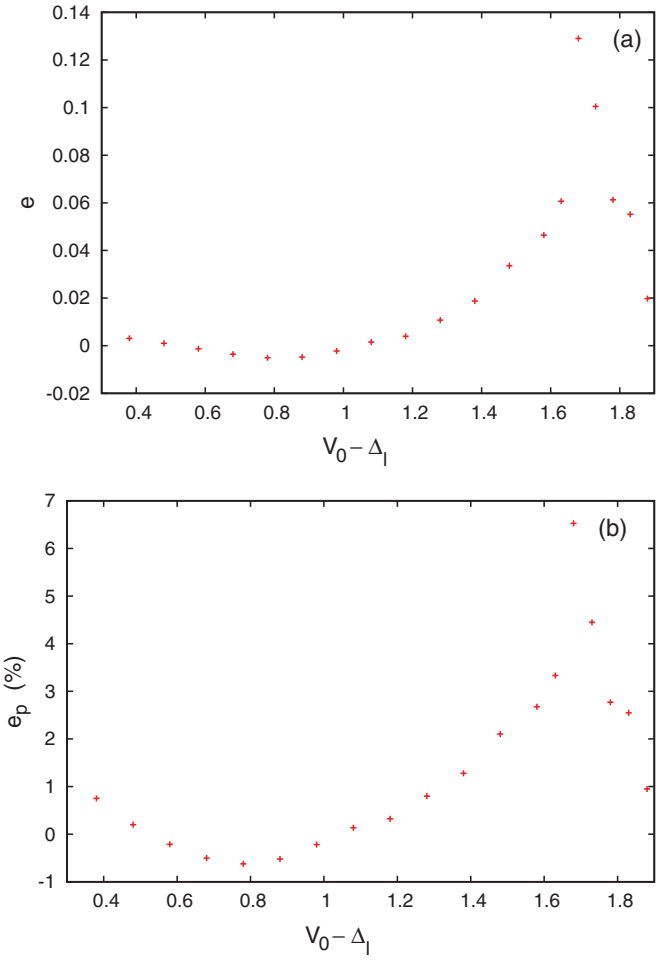

FIG. 5. (Color online) The error in the refracted propagation constant $V_f - \Delta_r$ as given by the modulation theory compared with the numerical solution as a function of the incident propagation constant $V_0 - \Delta_l$. The parameter values are $a = 5$ and $w = 2$, with $\nu = 200$, $\psi_{\rm bl} = 0.8$, $\psi_{\rm br} = 0.6$, $q_l = 1.3$, $q_r = 1.0$, $\mu_1 = 2.0$, and $\mu_2 = -8.0$. (a) Error e. (b) Percentage error e_p.

numerical value shown in Fig. 2. The difference between these two values is shown in Fig. 2(a) and the percentage error is shown in Fig. 2(b). The percentage error in the modulation propagation constant is generally less than 5%. The exception is for input $V_0 - \Delta_l$ between 0.05 and 0.3. This is because the refraction angle is 0 at $V_0 - \Delta_l = 0.1$, so that the percentage error is not a good measure of the difference around this input angle. While the refraction process for propagation into a more optically dense medium is nonlinear, in most respects it resembles linear, Snell-type refraction. Nonlinear effects become most apparent when propagation into a less optically dense medium is considered.

Let us now consider a solitary beam propagating from a more to a less optically dense medium. For such a change in optical density, a linear wave would either refract or undergo total internal reflection. However, a nematicon is an isolated, nonlinear wave packet with an extended transverse profile which results in a variety of possible behaviors, as schematically illustrated in Fig. 3. The nematicon can undergo refraction when passing into the less dense medium, type 1

TABLE I. $\mathcal{V}_0 = V_0 - \Delta_l$ ranges for refraction types to an optically less dense medium. The behavior types are classified as in Fig. 3. The parameter values are $a = 5$ and $w = 2$, with $\nu = 200$, $\psi_{\rm bl} = 0.8$, $\psi_{\rm br} = 0.6$, $q_l = 1.3$, $q_r = 1.0$, $\mu_1 = 2.0$, and $\mu_2 = -8.0$.

Refraction type	Numerical	Modulation
1	$\mathcal{V}_0 \leqslant 1.67$	$\mathcal{V}_0 \leqslant 1.709$
2	$1.68 \leqslant \mathcal{V}_0 < 1.812$	$1.71 \leqslant \mathcal{V}_0 < 1.800$
3	$\mathcal{V}_0 = 1.812$	$\mathcal{V}_0 = 1.800$
4	$1.812 < \mathcal{V}_0 \leqslant 2.02$	$1.800 < \mathcal{V}_0 \leqslant 2.019$
5	$\mathcal{V}_0 \geqslant 2.03$	$\mathcal{V}_0 \geqslant 2.020$

of Fig. 3, or proceed straight without a change in its trajectory if it does not approach the interface, type 5. For high angles of incidence, the nonlocal solitary wave shows three types of total internal reflection. The nematicon can enter the less dense medium, turn around, and reenter the more dense medium, resulting in Goos-Hänchen reflection [16,18,19,23,24,27], type 2 of Fig. 3. On increasing the angle of incidence, at a specific angle the nematicon undergoes total internal reflection with its axis exactly tangential to the interface, type 3 behavior. On further increase of the angle of incidence, the nematicon undergoes total internal reflection with its peak remaining in the denser medium, behavior type 4. In this case, reflection occurs due to the nematicon tail entering the less optically dense medium.

Figure 4 shows a comparison between the input and output propagation angles as given by the full numerical and modulation solutions. There is again excellent agreement, but an increasing difference as $V_0 - \Delta_l$ approaches 1.6, which is confirmed by the difference and percentage differences shown in Fig. 5. The propagation constant curve in Fig. 4 has a peak around $V_0 - \Delta_l = 1.85$. This peak is due to the nematicon changing from refraction to total internal reflection. A comparison between the ranges of $V_0 - \Delta_l$ for the different behaviors, illustrated schematically in Fig. 3, as given by the

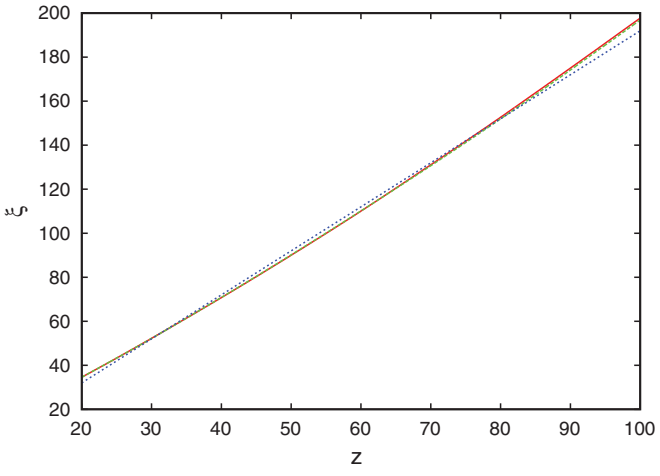

FIG. 6. (Color online) Comparison of trajectory ξ for an example of Goos-Hänchen reflection, behavior type 2 in Fig. 3. The parameter values are $a = 5$, $w = 2$ and $V_0 = 1.85$, with $\nu = 200$, $\psi_{\rm bl} = 0.8$, $\psi_{\rm br} = 0.6$, $q_l = 1.3$, $q_r = 1.0$, $\mu_1 = 2.0$ and $\mu_2 = -8.0$. Numerical solution,—(solid red line); modulation solution,– – –(dashed green line); interface, $\cdots$ (dotted blue line).

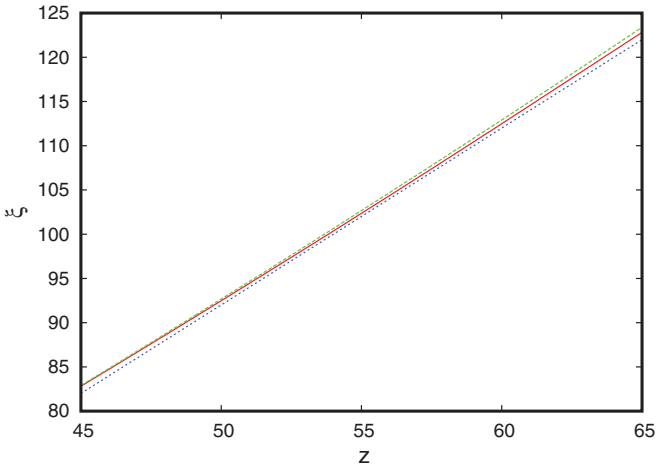

FIG. 7. (Color online) Comparison of trajectory ξ for an example of reflection in the denser medium, behavior type 4 in Fig. 3. The parameter values are $a = 5$, $w = 2$, and $V_0 = 1.95$, with $\nu = 200$, $\psi_{\rm bl} = 0.8$, $\psi_{\rm br} = 0.6$, $q_l = 1.3$, $q_r = 1.0$, $\mu_1 = 2.0$, and $\mu_2 = -8.0$. Numerical solution,—(solid red line); modulation solution,– – – (dashed green line); interface, $\cdots$ (dotted blue line).

modulation and numerical solutions is provided in Table I. Again, excellent agreement for the different regime ranges as predicted by the modulation solution is seen. Refraction changes to Goos-Hänchen reflection [16,18,19,23,24,27], type 2 of Fig. 3, at $V_0 - \Delta_l = 1.67$, with the beam passing through the interface, before bending back into the input region, as observed in experiments [16,23,24] and previous theoretical studies [18,19]. A typical case of Goos-Hänchen reflection is illustrated in Fig. 6. The agreement in the trajectories between the numerical and modulation solutions is excellent. At $V_0 - \Delta_l = 1.812$ Goos-Hänchen reflection stops and the nematicon undergoes total internal reflection exactly at the interface, type 3 of Fig. 3. After this value of V_0 the nematicon is totally internally reflected without its peak reaching the interface, as illustrated in Fig. 7, type 4 of Fig. 3. This is due to the interface being an extended (graded index) structure and the nematicon being a nonlocal solitary wave. Its tail can then enter the less optically dense medium, resulting in reflection, which gets weaker as a smaller portion of the tail enters the less dense medium, as shown by the smaller angle of reflection after $V_0 - \Delta_l = 1.812$ seen in Fig. 4. Eventually no change in trajectory occurs for $V_0 - \Delta_l \geqslant 2.03$ as there is insufficient overlap of the tail with the graded region to change the trajectory of the nematicon. It should be added that the total internal reflection of the nematicon is nonspecular due to the nonlinear response involved and to the anisotropy of the uniaxial medium with inherent walk-off, with the difference between the angles of incidence and reflection being up to about 2° for the example considered here, comparable to the 4.5° for experiments [23]. Of course, the exact value of the difference depends on the operating parameters used.

IV. CONCLUSIONS

The refraction of a nonlinear self-guided wave in nematic liquid crystals, a nematicon, at the interface between two regions with different director orientations, and hence refractive

indices, has been investigated using modulation theory. In previous experimental studies, these two orientations were produced by applying two different external voltages across the cell [16,23,24]. Our modulation theory is based on a Lagrangian formulation of the nematicon equations and their full numerical solutions. The angle of refraction is changed by altering the angle of incidence of the beam on the interface for a fixed external voltage difference, in contrast to experiments in which the beam was not tilted. Despite this difference, the present theoretical investigation reproduces the broad features of the experimental ones [16,23,24]. Similar changes in the propagation angle of the nematicon were found, ranging between -5° for refraction from a less to a more optically dense medium and $+10^\circ$ for total internal reflection from a more to a less optically dense medium. Excellent agreement was found between the full numerical solutions and the predictions of the modulation theory.

The most diverse range of refraction behavior was found for a beam propagating into a less optically dense medium. In analogy with linear wave refraction, total internal reflection can occur and take a number of forms. The beam axis can enter the less dense medium, refract, and reenter the more dense medium, so-called Goos-Hänchen reflection [18,19,27], as found in previous experimental studies [16,23,24]. The beam can also reflect without its peak entering the less dense medium, the refraction resulting from its tail interacting with the less dense medium. The reflection of the nematicon was found to be nonspecular, in accord with experimental results [23]. Excellent agreement was found between the ranges of these different types of refraction behavior as given by full numerical solutions and modulation theory.

This study of nematicon refraction fits in with a number of such studies which show the power and accuracy of modulation theory in giving simple, low-dimensional models in excellent agreement with numerical and experimental results [11,14,15,17].

ACKNOWLEDGMENT

This research was supported by the Royal Society of London under Grant No. JP090179.

APPENDIX A: MODULATION EQUATIONS

Taking variations of the averaged Lagrangian (9) results in the modulation equations describing the evolution of the nematicon:

$$\frac{d}{dz}(I_2 a^2 w^2 + \Lambda g^2) = 0, \tag{A1}$$

$$\frac{d\xi}{dz} = V - \frac{1}{2}[\Delta_l \operatorname{erfc}(\lambda_2) + \Delta_r \operatorname{erfc}(-\lambda_2)], \tag{A2}$$

$$\begin{aligned}\frac{dV}{dz} &= \frac{BV}{2\sqrt{\pi} I_2 w}(\Delta_l - \Delta_r)e^{-\lambda_2^2} \\ &+ \frac{AB\alpha\beta}{2\sqrt{\pi} I_2 w\sqrt{Q}}(\sin 2\psi_{\rm bl} - \sin 2\psi_{\rm br})e^{-\lambda_1^2} \\ &- \frac{\sqrt{2} D\alpha^2\beta}{4\sqrt{\pi} I_2 a^2 w^2}(q_l - q_r)e^{-\lambda_3^2},\end{aligned} \tag{A3}$$

$$I_1 \frac{d}{dz} a w^2 = \Lambda g\left(\sigma' - V\xi' + \frac{1}{2}V^2\right), \tag{A4}$$

$$\begin{aligned}I_1 \frac{dg}{dz} &= \frac{I_{22} a}{2w^2} - \frac{A^2 B^4 \alpha\beta^2 a w^2}{4Q^2}[\sin(2\psi_{\rm bl})\operatorname{erfc}(\lambda_1) \\ &+ \sin(2\psi_{\rm br})\operatorname{erfc}(-\lambda_1)] \\ &+ \frac{A^3 B\alpha\beta^3 a}{4\sqrt{\pi} w Q^{3/2}}[\sin 2\psi_{\rm bl} - \sin 2\psi_{\rm br}]e^{-\lambda_1^2} \\ &+ \frac{BaV}{4\sqrt{\pi} w}(\mu_1 z + \mu_2 - \xi)(\Delta_l - \Delta_r)e^{-\lambda_2^2},\end{aligned} \tag{A5}$$

$$\begin{aligned}&\frac{d\sigma}{dz} - V\frac{d\xi}{dz} + \frac{1}{2}V^2 \\ &= -\frac{I_{22}}{I_2 w^2} + \frac{A^2\alpha\beta^2(A^2\beta^2 + 2B^2 w^2)}{2Q^2}[\sin(2\psi_{\rm bl})\operatorname{erfc}(\lambda_1) \\ &+ \sin(2\psi_{\rm br})\operatorname{erfc}(-\lambda_1)] \\ &- \frac{A^3 B\alpha\beta^3}{4I_2 w Q^{3/2}}(\sin 2\psi_{\rm bl} - \sin 2\psi_{\rm br})e^{-\lambda_1^2} \\ &+ \frac{1}{2}V[\Delta_l \operatorname{erfc}(\lambda_2) + \Delta_r \operatorname{erfc}(-\lambda_2)] \\ &- \frac{BV}{4\sqrt{\pi} I_2 w}(\mu_1 z + \mu_2 - \xi)(\Delta_l - \Delta_r)e^{-\lambda_2^2},\end{aligned} \tag{A6}$$

together with the algebraic equations

$$\begin{aligned}\alpha &= \frac{A^2 B^2 \beta^2 a^2 w^2}{Q} \\ &\times \frac{\sin(2\psi_{\rm bl})\operatorname{erfc}(\lambda_1) + \sin(2\psi_{\rm br})\operatorname{erfc}(-\lambda_1)}{16\nu I_{42} + D^2\beta^2[q_l \operatorname{erfc}(\lambda_3) + q_r \operatorname{erfc}(-\lambda_3)]},\end{aligned} \tag{A7}$$

$$\begin{aligned}&\frac{A^2 B^4 \beta a^2 w^4}{Q^2}[\sin(2\psi_{\rm bl})\operatorname{erfc}(\lambda_1) + \sin(2\psi_{\rm br})\operatorname{erfc}(-\lambda_1)] \\ &+ \frac{AB^3 a^2 w^3}{\sqrt{\pi} Q^{3/2}}(\sin 2\psi_{\rm bl} - \sin 2\psi_{\rm br})(\mu_1 z + \mu_2 - \xi)e^{-\lambda_1^2} \\ &- \frac{1}{2}D^2\alpha\beta[q_l \operatorname{erfc}(\lambda_3) + q_r \operatorname{erfc}(-\lambda_3)] \\ &- \frac{D}{\sqrt{2\pi}}\alpha(q_l - q_r)(\mu_1 z + \mu_2 - \xi)e^{-\lambda_3^2} = 0.\end{aligned} \tag{A8}$$

The modulation equation (A1) is the equation for conservation of optical power, which is termed mass conservation in the sense of the scale invariance of the Lagrangian (7) [20]. The modulation equation (A3) is the equation for conservation of linear momentum. The trajectory of the beam is governed by this momentum equation and the modulation equation (A2). Unlike previous studies of the refraction of nematicons by changes in the liquid crystal medium, the trajectory equations (A2) and (A3) are not independent of the amplitude and width evolution of the nematicon as the position equations explicitly depend on the waist w of the nematicon via the complementary error functions in these equations [15]. The medium changes across the interface, so that the amplitude a and width w of the nematicon show significant adjustments.

The shelf radius R is given by Minzoni *et al.* [25]. However, due to the different scalings used in the nematicon equations (3) and (4), R must be replaced by $R\sqrt{2/\sin(2\psi_b)}$ and q must be replaced by $2q/\sin(2\psi_b)$ in Ref. [25].

APPENDIX B: INTEGRALS

The integrals I_i and $I_{i,j}$ in the modulation equations are

$$I_1 = \int_0^\infty \rho f(\rho)\, d\rho, \quad I_2 = \int_0^\infty \rho f^2(\rho)\, d\rho,$$
$$I_{22} = \int_0^\infty \rho \left[\frac{df}{d\rho}\right]^2 d\rho, \quad I_{x32} = \int_0^\infty \rho^3 f^2(\rho)\, d\rho,$$
$$I_{42} = \frac{1}{4}\int_0^\infty \rho \left[\frac{d}{d\rho} f^2(\rho)\right]^2 d\rho, \quad I_4 = \int_0^\infty \rho f^4(\rho)\, d\rho. \tag{B1}$$

For $f(\rho) = \operatorname{sech}\rho$,

$$I_1 = 2C, \quad I_2 = \ln 2, \quad I_{22} = \frac{1}{3}\ln 2 + \frac{1}{6},$$
$$I_{x32} = 1.352\,314\,016\ldots, \tag{B2}$$
$$I_{42} = \frac{2}{15}\ln 2 + \frac{1}{60}, \quad I_4 = \frac{2}{3}\ln 2 - \frac{1}{6}.$$

Here C is the Catalan constant $C = 0.915\,965\,594\ldots$ [32].

The constants A, B, and D arising in the modulation equations are

$$A = \frac{I_2\sqrt{2}}{\sqrt{I_{x32}}}, \quad B = \sqrt{2I_2}, \quad \text{and} \quad D = 2\sqrt{I_4}. \tag{B3}$$

[1] M. Peccianti, A. De Rossi, G. Assanto, A. De Luca, C. Umeton, and I. C. Khoo, Appl. Phys. Lett. **77**, 7 (2000).
[2] C. Conti, M. Peccianti, and G. Assanto, Phys. Rev. Lett. **91**, 073901 (2003).
[3] C. Conti, M. Peccianti, and G. Assanto, Phys. Rev. Lett. **92**, 113902 (2004).
[4] Yu. S. Kivshar and G. Agrawal, *Optical Solitons: From Fibers to Photonic Crystals* (Academic Press, San Diego, 2003).
[5] M. Peccianti, C. Conti, G. Assanto, A. de Luca, and C. Umeton, Appl. Phys. Lett. **81**, 3335 (2002).
[6] M. Peccianti, C. Conti, G. Assanto, A. de Luca, and C. Umeton, Nature (London) **432**, 733 (2004).
[7] S. V. Serak, N. V. Tabiryan, M. Peccianti, and G. Assanto, IEEE Photon. Tech. Lett. **18**, 1287 (2006).
[8] M. Peccianti, A. Dyadyusha, M. Kaczmarek, and G. Assanto, Phys. Rev. Lett. **101**, 153902 (2008).
[9] A. Piccardi, G. Assanto, L. Lucchetti, and F. Simoni, Appl. Phys. Lett. **93**, 171104 (2008).
[10] G. Assanto, A. Piccardi, A. Alberucci, S. Residori, and U. Bortolozzo, Photon. Lett. Poland **1**, 151 (2009).
[11] G. Assanto, B. D. Skuse, and N. F. Smyth, Photon. Lett. Poland **1**, 154 (2009).
[12] A. Alberucci, A. Picardi, U. Bortolozzo, S. Residori and G. Assanto, Opt. Lett. **35**, 390 (2010).
[13] A. Piccardi, A. Alberucci, U. Bortolozzo, S. Residori, and G. Assanto, Appl. Phys. Lett. **96**, 071104 (2010).
[14] G. Assanto, B. D. Skuse, and N. F. Smyth, Phys. Rev. A **81**, 063811 (2010).
[15] G. Assanto, A. A. Minzoni, N. F. Smyth, and A. L. Worthy, Phys. Rev. A **82**, 053843 (2010).
[16] M. Peccianti, A. Dyadyusha, M. Kaczmarek, and G. Assanto, Nat. Phys. **2**, 737 (2006).
[17] G. Assanto, A. A. Minzoni, M. Peccianti, and N. F. Smyth, Phys. Rev. A **79**, 033837 (2009).
[18] A. B. Aceves, J. V. Moloney, and A. C. Newell, Phys. Rev. A **39**, 1809 (1989).
[19] A. B. Aceves, P. Varatharajah, A. C. Newell, E. M. Wright, G. I. Stegeman, D. R. Heatley, J. V. Moloney, and H. Adachihara, J. Opt. Soc. Am. B **7**, 963 (1990).
[20] D. J. Kaup and A. C. Newell, Proc. R. Soc. London A **361**, 413 (1978).
[21] J. Sánchez-Curto, P. Chamorro-Posada, and G. S. McDonald, Phys. Rev. A **83**, 013828 (2011).
[22] A. Piccardi, A. Alberucci, N. Tabiryan, and G. Assanto, Opt. Lett. **36**, 1356 (2011).
[23] M. Peccianti, G. Assanto, A. Dyadyusha, and M. Kaczmarek, Phys. Rev. Lett. **98**, 113902 (2007).
[24] M. Peccianti, G. Assanto, A. Dyadyusha, and M. Kuczmarek, Opt. Lett. **32**, 271 (2007).
[25] A. A. Minzoni, N. F. Smyth, and A. L. Worthy, J. Opt. Soc. Am. B **24**, 1549 (2007).
[26] B. D. Skuse and N. F. Smyth, Phys. Rev. A **77**, 013817 (2008).
[27] F. Goos and H. Hänchen, Ann. Phys. **436**, 333 (1947).
[28] M. Peccianti, A. Fratalocchi, and G. Assanto, Opt. Express **12**, 6524 (2004).
[29] C. García-Reimbert, A. A. Minzoni, N. F. Smyth, and A. L. Worthy, J. Opt. Soc. Am. B **23**, 2551 (2006).
[30] W. L. Kath and N. F. Smyth, Phys. Rev. E **51**, 1484 (1995).
[31] G. B. Whitham, *Linear and Nonlinear Waves* (Wiley & Sons, New York, 1974).
[32] M. Abramowitz and I. A. Stegun, *Handbook of Mathematical Functions with Formulas, Graphs and Mathematical Tables* (Dover, New York, 1972).
[33] B. Fornberg and G. B. Whitham, Philos. Trans. R. Soc. London A **289**, 373 (1978).